Equivalent-Circuit Models for the Design of Metamaterials Based on Artificial Magnetic Inclusions

Filiberto Bilotti, *Senior Member, IEEE*, Alessandro Toscano, *Member, IEEE*, Lucio Vegni, *Member, IEEE*, Koray Aydin, *Student Member, IEEE*, Kamil Boratay Alici, and Ekmel Ozbay

***Abstract*—In this paper, we derive quasi-static equivalent-circuit models for the analysis and design of different types of artificial magnetic resonators—i.e., the multiple split-ring resonator, spiral resonator, and labyrinth resonator—which represent popular inclusions to synthesize artificial materials and metamaterials with anomalous values of the permeability in the microwave and millimeter-wave frequency ranges. The proposed models, derived in terms of RLC equivalent circuits, represent an extension of the models presented in a recent publication. In particular, the extended models take into account the presence of a dielectric substrate hosting the metallic inclusions and the losses due to the finite conductivity of the conductors and the finite resistivity of the dielectrics. Exploiting these circuit models, it is possible to accurately predict not only the resonant frequency of the individual inclusions, but also their quality factor and the relative permeability of metamaterial samples made by given arrangements of such inclusions. Finally, the three models have been tested against full-wave simulations and measurements, showing a good accuracy. This result opens the door to a quick and accurate design of the artificial magnetic inclusions to fabricate real-life metamaterial samples with anomalous values of the permeability.**

***Index Terms*—Artificial magnetic inclusions, labyrinth resonators, metamaterials, miniaturization, multiple split-ring resonators, split-ring resonators.**

I. Introduction

ARTIFICIAL materials exhibiting anomalous values of the permeability, (e.g., materials with values of the relative permeability greater than one [1], with negative values of the permeability: the so-called mu-negative materials [2], with a zero value of the permeability, with an absolute value of the relative permeability less than one: the so-called mu-near-zero materials [3]) are of interest in many applications at different frequency ranges.

Such materials are usually obtained at microwaves by printing suitable metallic resonating inclusions on supporting dielectric boards and stacking the boards to form a *medium*. The inclusions react to the impinging magnetic field, and provided that the dimensions of and the separation between the inclusions are small compared to the wavelength, the magnetic response of the artificial material can be expressed in terms of a macroscopic permeability function [4]–[6].

In most cases, the main reason to employ artificial magnetic metamaterials in the design of transmissive and radiating microwave components is related to the possibility of squeezing the component dimensions [6]–[10] by using electrically small samples of artificial magnetic materials (planar slabs, cylindrical shells, rods, etc.). Since in some cases [6]–[9] there is no theoretical limitation for the achievable miniaturization (i.e., the dimensions of the materials can be, in principle, even infinitesimal), the only intrinsic limit is represented by the dimensions of the inclusions used to fabricate the needed metamaterial samples. However, the most common type of resonator used to achieve anomalous values of the permeability at microwaves, the split-ring resonator [11], exhibits a physical dimension of the order of $\lambda/20$, which may represent, thereby, a significant limitation.

In order to overcome this drawback and reduce the dimensions of the resonant inclusions, multiple split-ring and spiral resonators may be used. In [12], we have presented suitable LC circuit models for a quick design of both of these artificial magnetic inclusions. Such models are limited to the ideal cases of: 1) absence of losses and 2) resonators immersed in air. Moreover, the models presented in [12] are able to accurately predict only the resonant frequency of the individual inclusions without giving any information about their quality factor, which may give a good indication of the bandwidth of operation of the metamaterial constituted by those inclusions. Finally, the LC circuit models proposed in [12] do not give the designer any information on how to get a specific value of the real part of the permeability needed to fabricate a given component and on the losses related to the imaginary part of the permeability in realistic layouts.

The aim of this paper is to present a significant extension of the work done in [12], proposing complete circuit models that also take into account the presence of a dielectric substrate where the inclusions are printed on and the losses both in the dielectrics and metallic conductors. Moreover, in this paper, we compare the analytical results obtained from the presented models and both the full-wave simulations and measurements.

On the other hand, when moving towards higher microwave frequencies, miniaturization of the inclusions might not be an

Manuscript received May 2, 2007; revised July 27, 2007. This work was supported by the European Union under the Network of Excellence METAMORPHOSE.

F. Bilotti, A. Toscano, and L. Vegni are with the Department of Applied Electronics, University of "Roma Tre," Rome 00146, Italy (e-mail: bilotti@uniroma3.it).

K. Aydin, K. B. Alici, and E. Ozbay are with the Department of Physics and the Department of Electrical and Electronics Engineering, Nanotechnology Research Center, Bilkent University, Bilkent 06800, Turkey.

Color versions of one or more of the figures in this paper are available online at http://ieeexplore.ieee.org.

Digital Object Identifier 10.1109/TMTT.2007.909611

issue any more. Sometimes, indeed, miniaturization has to be avoided, due to the technological limitations to print sufficiently small inclusions. In this case, new concepts have to be employed in the design of the inclusions and a possible solution consists in the employment of the so-called labyrinth resonators [13], i.e., inclusions characterized by multiple splits along the ring strips. The labyrinth resonator has been experimentally investigated in [13], while in [14], for the first time, we have derived an accurate analytical model of this type of inclusion based again on a suitable LC resonant circuit. Also in this case, the model is limited to a labyrinth resonator immersed in air and made by an ideal conductor. In this paper, we extend the formulation presented in [14] and propose a complete model, which takes into account the presence of the dielectric substrate and the losses in the conductors and dielectrics. Also in this case, the analytical model is tested through a proper comparisons with full-wave numerical results and the measurements.

This paper is organized as follows. In Section II, we present the extended analytical models of the multiple split-ring, spiral, and labyrinth resonators in terms of suitable RLC equivalent circuits, validated through the comparison with proper full-wave numerical simulations and experimental measurements. In Section III, we analytically derive the quality factor of the isolated inclusions proposed in Section II. A discussion of the quality factor is also conducted with the perspective of the possible applications in real-life artificial magnetic metamaterials. Finally, an analytical representation of the macroscopic permeability function of a given arrangement of resonators is derived and compared with the permeability numerically retrieved through the scattering parameters [15], [16].

II. Multiple Split-Ring, Spiral, and Labyrinth Resonators: Analytical Model, Design, and Experimental Verification

A. Multiple Split-Ring Resonators

In [12], it has been shown that the electromagnetic behavior in the quasi-static regime (i.e., when the inclusions are much smaller than the operating wavelength, which is, indeed, the case when artificial magnetic inclusions are used to fabricate metamaterial samples) of the lossless multiple split-ring resonator immersed in air is described by the equivalent LC series circuit depicted in [12, Fig. 1(b)].

The presence of a dielectric substrate, upon which the multiple split-ring resonator is printed [see Fig. 1(a)], does not affect the inductance. Therefore, its expression is the same as the one reported in [12]

$$L^{\mathrm{MSRR}} = \frac{\mu_0}{2}\frac{\ell_{\mathrm{avg}}}{4}4.86\left[\ln\left(\frac{0.98}{\rho}\right)+1.84\rho\right] \tag{1}$$

where μ_0 is the vacuum permeability, ℓ is the side length of the external ring, w is the width of the strips, s is the separation between two adjacent strips, $\ell_{\mathrm{avg}} = 4[\ell-(N-1)(w+s)]$ is the average strip length calculated over all the N rings, and $\rho = (N-1)(w+s)/[\ell-(N-1)(w+s)]$ is the so-called filling ratio [12].

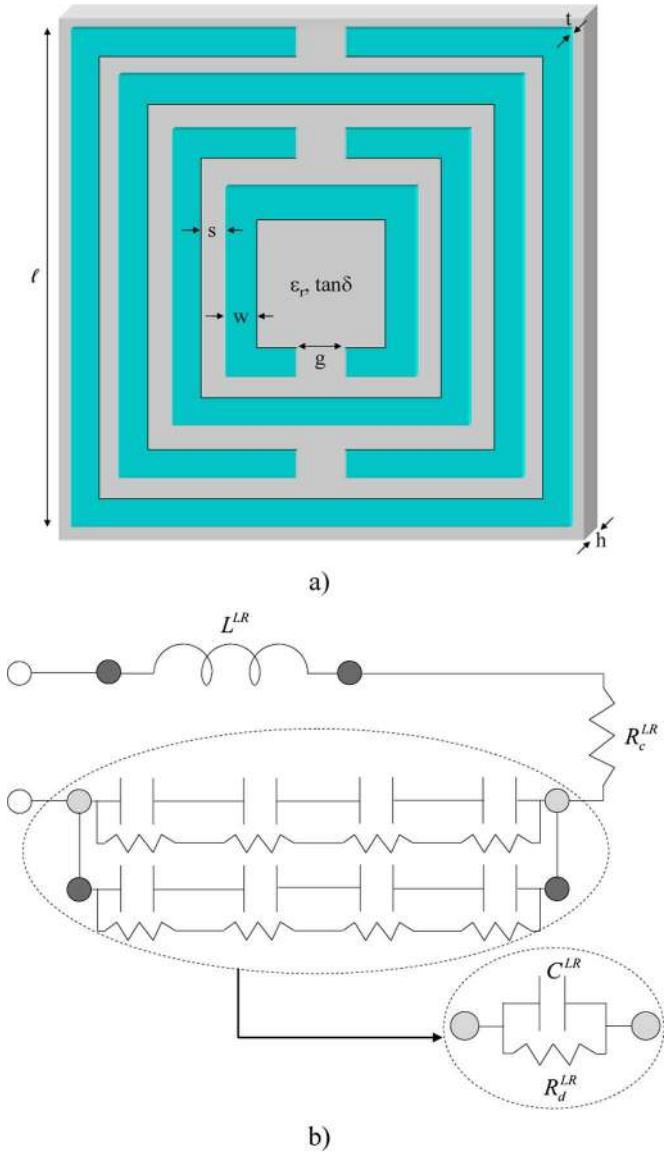

Fig. 1. (a) Sketch and geometrical dimensions of a multiple split-ring resonator. (b) Quasi-static equivalent circuit model of the multiple split-ring resonator depicted in (a).

The expression of the capacitance is also given by the formula derived in [12]

$$C^{\mathrm{MSRR}} = \frac{N-1}{2}[2\ell-(2N-1)(w+s)]C_0 \tag{2}$$

but this time, the per-unit-length capacitance between two parallel strips having width w and separation s in the presence of a dielectric substrate of height h and relative permittivity ε_r differs from the one given in [12] and reads

$$C_0 = \varepsilon_0\varepsilon_r^{\mathrm{sub}}(\varepsilon_r,h,w,s)\frac{K(\sqrt{1-k^2})}{K(k)} \tag{3}$$

where ε_0 is the vacuum permittivity, K is the complete elliptic integral of the first kind, $k = s/(s+2w)$, and the effective relative permittivity $\varepsilon_r^{\mathrm{sub}}$ related to the dielectric filling the substrate is given by

$$\varepsilon_r^{\mathrm{sub}}(\varepsilon_r,h,w,s) = 1+\frac{2}{\pi}\mathrm{arctg}\left[\frac{h}{2\pi(w+s)}\right](\varepsilon_r-1). \tag{4}$$

This formula has been heuristically determined through a proper fit of different sets of numerical data under the assumption that the substrate thickness h is not very large compared to the inclusion details (i.e., $0 \leq (h/w),(h/s) < 12\pi$).[1] In particular, four constraints have been imposed to derive (4), which are: 1) when $0 \leq (h/w),(h/s) \ll 1$, the effective permittivity is expected to be a linear function of $h/w, h/s$; 2) a further increase of the substrate thickness should correspond to a smoother growing of the effective permittivity; 3) $\varepsilon_r^{\rm sub}$ should go to 1 when the thickness h of the dielectric substrate vanishes; and 4) $\varepsilon_r^{\rm sub}$ should go to 1 when the substrate is filled by air. Formula (4) satisfies all four of these constraints in the range of validity.

Although mutual interactions between nonadjacent segments and rings are neglected, (1) and (2) describe in an accurate manner the behavior of the multiple split-ring resonator in the quasi-static limit when perfect conductors and dielectrics are considered [12].

In the case of lossy conductors and dielectrics, the correct equivalent circuit of the multiple split-ring resonator is now the one reported in Fig. 1(b). We added a series resistance $R_c^{\rm MSRR}$ to take into account the losses in the conductor and a shunt resistance $R_d^{\rm MSRR}$ to describe the losses in the dielectric substrate.

The equivalent resistance $R_c^{\rm MSRR}$ is in series with the inductance $L^{\rm MSRR}$ and, thus, should be calculated along the same domain (i.e., the equivalent loop described in [12]). Inductance $L^{\rm MSRR}$ in (1) can be cast in the form $L^{\rm MSRR} = L_0 \ell_{\rm avg}(\rho)$, where $L_0 = \mu_0$ is a per-unit-length inductance and $\ell_{\rm avg}(\rho) = \ell_{\rm avg} f(\rho)$ is the average length of the loop with $f(\rho)$ being a correction function depending on the filling ratio. Therefore, the total series resistance can be cast in the same form as $R_c^{\rm MSRR} = R_0 \ell_{\rm avg}(\rho)$, where $R_0 = (\rho_c/wt)$ is the per-unit-length resistance, with ρ_c being the electrical resistivity of the metal and t being the thickness of the metallic strips. Thereby, the final expression of the total series resistance reads

$$R_c^{\rm MSRR} = \frac{\rho_c}{wt}\frac{L^{\rm MSRR}}{\mu_0}. \tag{5}$$

The shunt resistance $R_d^{\rm MSRR}$ is in parallel with the total capacitance $C_d^{\rm MSRR}$ and can be determined as follows. Let us consider at first the most external pair of rings. Following the discussion about the current and voltage distribution on the rings referred in [12], the conductances associated to the two symmetrical halves of the ring pair are connected in series to each other. Therefore, the total conductance of the most external pair of rings is given by $G' = G_0 \ell'/4$, where $\ell' = 4\ell - 4(2w+s)$ is the total length of the gap between the two rings and $G_0 = \sigma_d h/s$ is the per-unit-length conductance, with σ_d being the conductivity of the dielectric substrate. The shunt resistance associated to the most outer pair of rings is thus given by $R' = 4(1/\sigma_d)(s/h\ell')$. When adding the other inner rings, the shunt resistances associated to each pair of adjacent rings are all connected in parallel. However, since these resistances are not equal to each other, due to the different lengths of the rings, it is not straightforward to derive a formula for the total equivalent shunt resistance $R_d^{\rm MSRR}$. We just know that this resistance should have the form $R_d^{\rm MSRR} = R' g(N)$, with $g(N)$ being a decreasing function of N. Under the assumption that N is not too close to the maximum number of the rings allowable for a given inclusion,[2] a suitable expression for $g(N)$ has been determined through a proper fitting of numerical data as $g(N) = (\ell_{\rm avg}/4\ell)$. Therefore, the final expression for $R_d^{\rm MSRR}$ is given by

$$R_d^{\rm MSRR} = \frac{1}{\sigma_d}\frac{s}{h[\ell-(2w+s)]}\frac{\ell_{\rm avg}}{4\ell}. \tag{6}$$

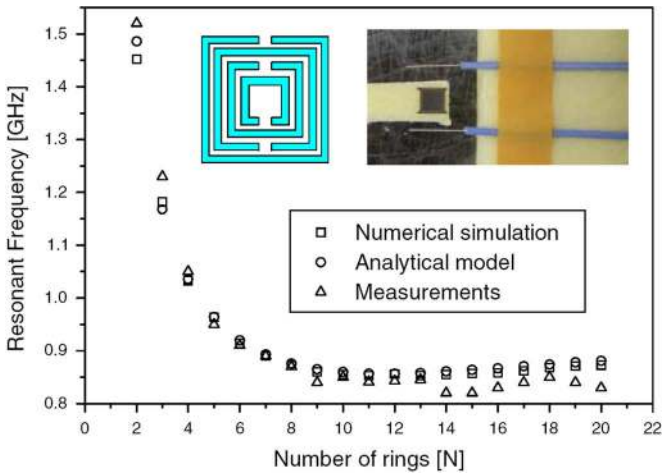

Fig. 2. Resonant frequency of a multiple split-ring resonator as a function of the number of rings N. In the inset, we show the experimental setup used to measure the transmission features and, thus, the resonant frequency of the isolated inclusion. Data: $\ell = 8$ mm, $w = 0.1$ mm, $s = 0.1$ mm, $t = 30$ μm, $h = 0.2$ mm, $\varepsilon_r = 3.85, \tan\delta = 0.01, \rho_c = 0.017 \cdot 10^{-6}$ Ωm.

Using (1)–(6) and the circuit representation depicted in Fig. 1(b), it is now possible to analytically calculate the resonant frequency of the individual inclusion. The comparison with the values obtained through the full-wave numerical results performed through CST Microwave Studio and the measurements is reported in Fig. 2.

The inset of Fig 2 shows how the measurements have been performed. As already done in [13] for a different type of resonator, the isolated multiple split-ring resonator has been placed between two electrically small monopole antennas connected to the HP-8510C network analyzer to measure the transmission coefficient. The antennas and resonator are arranged in such a way that the magnetic field produced in the near zone by the antennas excites the multiple split-ring resonator (see the inset of Fig. 2). In order to calibrate the network analyzer, we measured at first the transmission spectra in free space (i.e., without the multiple split-ring resonator unit cell). We then have inserted the multiple split-ring resonator unit cell between the monopole antennas, and we performed the transmission measurements by maintaining the distance between the transmitter and receiver monopole antennas fixed.

[1]When talking about metamaterials, in fact, we should keep in mind that the separation between the inclusions is assumed to be much smaller than the wavelength, as it happens also for the inclusion dimensions.

[2]The reader may find in [12] a quantitative definition of the maximum number of rings that a given inclusion can host. It should be noticed that the assumption adopted here is in line with the practical employment of the inclusions in metamaterial samples. As already pointed out in [12] and later in this paper, the number N of the rings to be used depends on the filling ratio and it is far from the maximum.

The numerical simulation of the behavior of the inclusion has been performed in two ways, which are: 1) we have considered a plane wave impinging on the isolated inclusion depicted in Fig. 1(a) with the impinging magnetic field aligned along the axis of the magnetic inclusion (in this case, in order to detect the magnetic resonant frequency of the inclusion, a magnetic field probe revealing the normal component of the H-field with respect to the multiple split-ring resonator has been placed in the center of the inclusion) and 2) we have simulated the experimental setup previously described with the two antennas and the multiple split-ring resonator in the middle). The simulations performed through these two methods return very close values of the resonant frequency (the discrepancy is always within a couple of percentage points).

The good agreement between measured, simulated, and analytical data is well evident from Fig. 2. In addition, in Fig. 2, the expected saturation of the resonant frequency (see [12]) is also evident. From the practical point of view, we learn that a few rings are enough to obtain a good reduction of the resonant frequency, giving a typical miniaturization rate of the order of $\lambda/40 - \lambda/50$ in the linear dimensions of the inclusion.

B. Spiral Resonators

Further miniaturization may be obtained using the spiral resonator [17], [18] depicted in Fig. 3(a). Such an inclusion, which is the planar version of the "Swiss roll" (i.e., a metallic sheet wound as a coil to form a cylindrical resonator) proposed in [11] is currently used in several experimental layouts (including low-profile antennas [19] and ultrathin microwave absorbers [20]) that foresee the employment of magneto-dielectrics and mu-negative metamaterials.

In parallel to what has been done for the multiple split-ring resonator, we have already derived in [12] an accurate LC equivalent model for the lossless isolated spiral resonator immersed in air. The presence of a dielectric substrate affects only the distributed capacitance between the turns of the spiral and, thus, the final expressions of the total inductance and capacitance read as follows:

$$L^{\mathrm{SR}} = \frac{\mu_0}{2\pi}\ell_{\mathrm{avg}}^{\mathrm{SR}}\left[\ln\left(\frac{\ell_{\mathrm{avg}}^{\mathrm{SR}}}{2w}\right)+\frac{1}{2}\right] \tag{7}$$

$$C^{SR} = \frac{\ell}{4(w+s)}\frac{N^2}{N^2+1} \times\left[\ell(N-1)-\frac{N^2-1}{2}(w+s)\right]C_0 \tag{8}$$

where this time N is the number of the turns of the spiral, ℓ is the side length of the external turn, w is the width of the strips, s is the separation between two adjacent turns, C_0 is defined as for the multiple split-ring resonator, and $l_{\mathrm{avg}}^{\mathrm{SR}} = 4\ell - [2(N+1) - 3/N](s+w)$ is the average length of the spiral turn.

It is worth noticing that, as in the case of the multiple split-ring resonator, we have also considered in this case the squared version of the spiral resonator. Anyway, the same formulation also applies to the circular counterparts, simply by changing the length of the straight segments with the length of the circular ones.

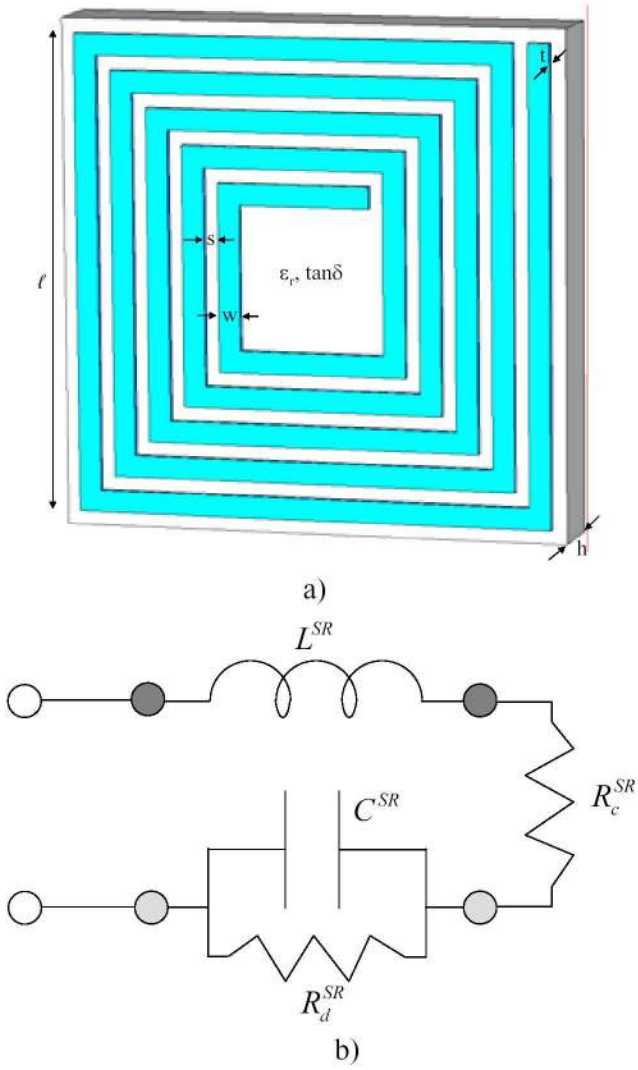

Fig. 3. (a) Sketch and geometrical dimensions of a spiral resonator. (b) Quasi-static equivalent circuit model of the spiral resonator depicted in Fig. 3(a).

Now assuming the presence of the losses in the metallic conductor and in the dielectric, the equivalent-circuit model of the spiral resonator is the one depicted in Fig. 3(b). The series resistance taking into account the losses in the conductor has been determined analogously to the multiple split-ring resonator case and it is given by

$$R_c^{\mathrm{SR}} = \frac{\rho_c}{wt}\frac{L^{\mathrm{SR}}}{\mu_0}. \tag{9}$$

In the same way, the shunt resistance, which takes into account the dissipation in the lossy dielectric, can be written as

$$R_d^{\mathrm{SR}} = \frac{1}{\sigma_d}\frac{s}{4h[\ell-(2w+s)]}\frac{\ell_{\mathrm{avg}}^{\mathrm{SR}}}{4\ell}. \tag{10}$$

Also in this case, from the equivalent circuit depicted in Fig. 3 and (7)–(10), it is possible to analytically derive the resonant frequency of the spiral resonator. A comparison between the results obtained using the proposed analytical model, the full-

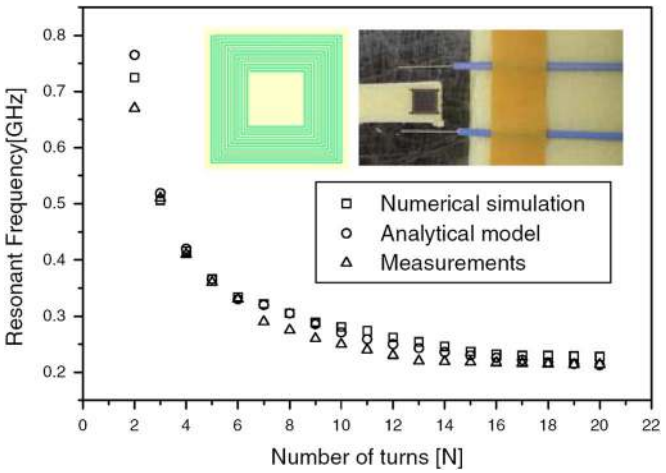

Fig. 4. Resonant frequency of a spiral resonator as a function of the number of the turns N. Data: $\ell = 8$ mm, $w = 0.1$ mm, $s = 0.1$ mm, $t = 30\ \mu$m, $h = 0.2$ mm, $\varepsilon_r = 3.85, \tan\delta = 0.01, \rho_c = 0.017 \cdot 10^{-6}\ \Omega$m.

wave simulations carried out through CST, and the measurements is reported in Fig. 4. A good agreement between the different sets of data is observed.

Please also note in this case the saturation behavior obtained when increasing the number of the turns. Again, there is no need to fill in the entire free area in the center of the resonator. The achievable miniaturization here is of the order of $\lambda/170$, which is a useful result for a lot of interesting applications.

C. Labyrinth Resonators

When metamaterials with anomalous values of the permeability are to be designed for the higher microwave frequencies, miniaturization is not always desired. To this end, a suitable inclusion, called the labyrinth resonator, has been proposed in [13]. The details on how to derive from the circuit model the total inductance and capacitance when the inclusion is in free space and losses are neglected have already been reported in [14].

The inductance is not affected by the presence of the dielectric substrate [see Fig. 5(a)] and should be the same as in [14]. However, we found out that, in parallel to what happens for the multiple split-ring and spiral resonators [see (1) and (7)], it is better to replace the total external length of the inclusion 4ℓ with the average length of the ring as

$$L^{\mathrm{LR}} = \frac{\mu_0}{2}\frac{\ell_{\mathrm{avg}}^{\mathrm{LR}}}{4}\left[\ln\left(\frac{\ell_{\mathrm{avg}}^{\mathrm{LR}}}{w}\right) - 2\right]. \tag{11}$$

The total capacitance of the labyrinth resonator is given by two contributions, which are: 1) the distributed capacitance as for the previous inclusions and 2) the capacitances associated to the cuts. In the case of the labyrinth resonator, in fact, it is not advised to neglect the cut capacitances anymore. Since the effect of the distributed capacitance is very much reduced in the labyrinth resonator, the length of the gap g starts playing a significant role. The gap capacitance, in fact, may be of the same order of magnitude of the total distributed capacitance.

Considering the series and parallel connections of the capacitances in Fig. 5(b), the first contribution is given by the sum of

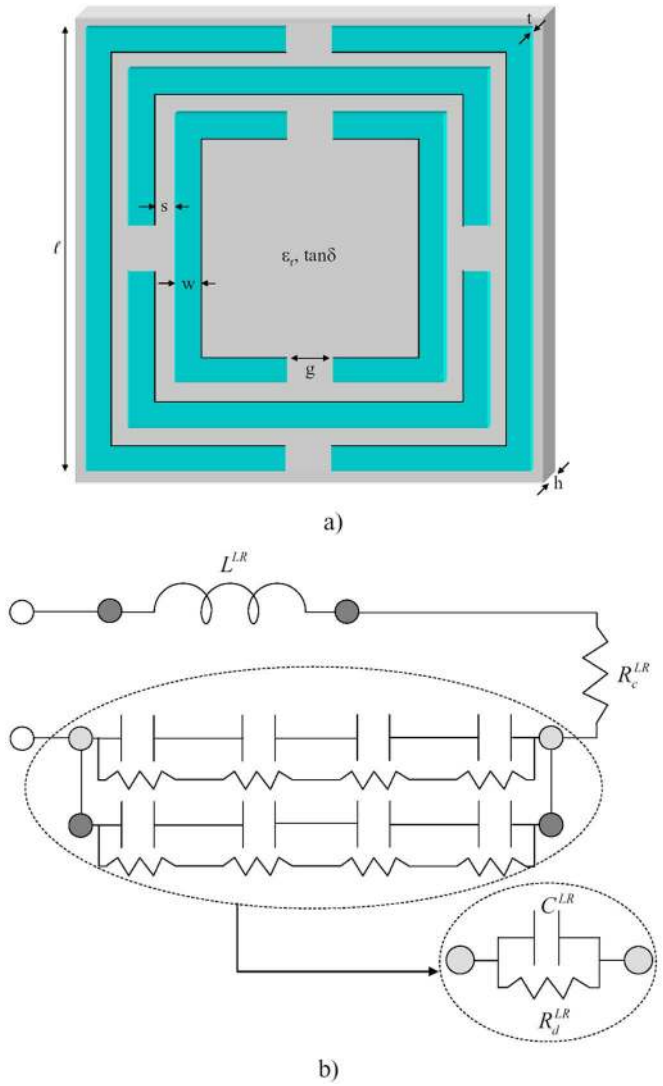

Fig. 5. (a) Sketch and geometrical dimensions of a labyrinth resonator. (b) Quasi-static equivalent-circuit model of the labyrinth resonator depicted in (a).

the distributed capacitances between any pair of adjacent rings as

$$C_1^{\mathrm{LR}} = \frac{C_0}{16}\left\{(N-1)\left[4(\ell - g) - \frac{N}{2}(s+2w)\right]\right\} \tag{12}$$

where this time N is the number of the concentric rings, ℓ is the side length of the external ring, w is the width of the strips, s is the separation between two adjacent rings, g is the length of the cuts, and C_0 is defined as for the multiple split-ring and the spiral resonator.

The second contribution, instead, is given by the sum of the capacitances of the $2N$ gaps as

$$C_2^{\mathrm{LR}} = 2N\varepsilon_0\varepsilon_r^{\mathrm{sub}}(\varepsilon_r, h, w, s)\frac{2w+\sqrt{2}g}{\pi}\operatorname{arccosh}\left[\frac{2w+g}{g}\right] \tag{13}$$

where the usual formula of the capacitance between two printed strips with separation g and width w has been amended here by using (4).

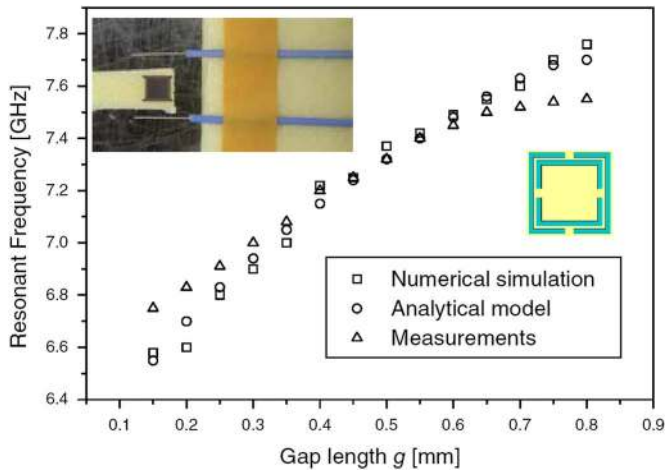

Fig. 6. Resonant frequency of a labyrinth resonator as a function of the gap length g. Data: $\ell = 5.65$ mm, $w = 0.9$ mm, $s = 0.2$ mm, $t = 30\ \mu$m, $h = 1.6$ mm, $\varepsilon_r = 3.85, \tan\delta = 0.01, \rho_c = 0.017 \cdot 10^{-6}\ \Omega$m.

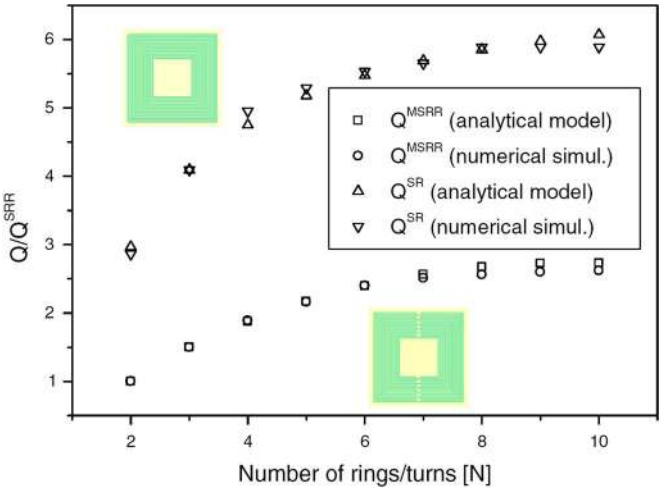

Fig. 7. Quality factor of individual multiple split-ring and spiral resonators as a function of the number of the rings/turns N. The quality factor is normalized to the one of the split-ring resonator with the same space occupancy (i.e., the multiple split-ring resonator with $N = 2$). Simulated results are from [12]. Data: $\ell = 5$ mm, $w = 0.1$ mm, $s = 0.1$ mm, $t = 30\ \mu$m, $h = 0.2$ mm, $\varepsilon_r = 1.01, \tan\delta = 0.001, \rho_c = 0.017 \cdot 10^{-6}\ \Omega$m.

Finally, since it can be shown that the gap capacitance is connected in parallel to the distributed capacitance [11], the total capacitance is given by

$$C^{\mathrm{LR}} = C_1^{\mathrm{LR}} + C_2^{\mathrm{LR}}. \tag{14}$$

The series resistance of the labyrinth resonator is obtained in the same way as for the previous inclusions as

$$R_c^{\mathrm{LR}} = \frac{\rho_c}{wt}\frac{L^{\mathrm{LR}}}{\mu_0}. \tag{15}$$

The shunt resistance is instead given by the two following contributions:

$$R_{d1}^{\mathrm{LR}} = \frac{1}{\sigma_d}\frac{\ell_{\mathrm{avg}}^{\mathrm{SR}}}{4\ell}\frac{s}{h[4\ell - 4(2w+s) - 2g]} \tag{16}$$

$$R_{d2}^{\mathrm{LR}} = \frac{1}{\sigma_d}\frac{g}{2hwN} \tag{17}$$

where the average length of the ring reads

$$l_{\mathrm{avg}}^{\mathrm{LR}} = 4\ell - 2g - (N-1)(s+w). \tag{18}$$

R_{d1}^{LR}, which is the resistance associated to the dielectric losses between the strips, has been calculated as for the multiple split-ring and the spiral resonator, while R_{d2}^{LR}, which represents the dielectric losses in the cuts, is derived straightforwardly from the definition of resistance and considering that all the $2N$ contributions are equal and all connected in parallel. The final expression of the equivalent shunt resistance thus reads

$$R_d^{\mathrm{LR}} = \frac{R_{d1}^{\mathrm{LR}} R_{d2}^{\mathrm{LR}}}{R_{d1}^{\mathrm{LR}} + R_{d2}^{\mathrm{LR}}}. \tag{19}$$

Again, using the equivalent circuit depicted in Fig. 5(b) and (11)–(14), it is possible to analytically derive the resonant frequency of the individual labyrinth resonator. In Fig. 6, we show the comparison between the results obtained through the model proposed here, CST full-wave simulations, and measurements.

III. Quality Factor and Permeability Function

A. Quality Factor of the Isolated Inclusion

One of the main issues related to real-life metamaterials is their inherent narrow bandwidth of operation. The bandwidth of the fabricated metamaterial is strongly related to the resonance behavior of the inclusions used to implement the material. Since the resonant behavior of the inclusions can be easily derived from the accurate resonant circuits we have presented in Section II, it is also possible to analytically express the expected operative bandwidth of a metamaterial made up by a certain set of inclusions.

A good estimation of the bandwidth may be derived as the inverse of the quality factor Q related to the resonance of the individual inclusion. Considering generic equivalent RLC circuit representations as the ones proposed in Section II, the quality factor Q in the presence of the losses both in the dielectric substrate and metallic conductor can be written as [21]

$$\frac{1}{Q} = \frac{1}{Q_c} + \frac{1}{Q_d} \tag{20}$$

where Q_c is the quality factor related to the losses in the metallic conductor and is given by

$$Q_c = \omega_{0A}\frac{L^A}{R_c^A}, \qquad \text{with } A = \mathrm{MSRR}, \mathrm{SR}, \mathrm{LR}. \tag{21}$$

Q_d is the quality factor related to the losses in the dielectric substrate and is given by

$$Q_d = \omega_{0A} R_c^A C^A, \qquad \text{with } A = \mathrm{MSRR}, \mathrm{SR}, \mathrm{LR} \tag{22}$$

with $\omega_{0A} = 1/\sqrt{L^A C^A}$ being the angular resonant frequency of the circuit.

In Fig. 7, we show the behavior of the quality factor of individual multiple split-ring and spiral resonators as a function

of the number of rings/turns N. The quality factor is normalized to the one of the split-ring resonator with the same space occupancy.

The comparison between the analytical evaluation of the quality factor using the proposed circuit models and the numerical results presented in [12] clearly shows the accuracy of the present formulation.

It is worth noticing that, as expected, in the cases of multiple split-ring and spiral resonators, the electrically smaller the inclusions (i.e., the higher the miniaturization rate is), the higher the Q and the narrower the operation bandwidth of the metamaterial. This is, of course, an unavoidable optimization issue, whose solution is left to the designer and depends on the specific application for which the metamaterial has to be tailored.

B. Equivalent-Circuit Model and Permeability Function

Here we present a compact and accurate formulation for the effective permeability of a medium densely filled with multiple split-ring, spiral, and labyrinth resonators. As a first-order approximation, the permeability function is derived using the Clausius–Mosotti [10] equation as

$$\mu_{\text{eff}} = \mu_0 \left(1 + \frac{n\alpha_{mm}}{1 - \dfrac{n\alpha_{mm}}{3}} \right) \tag{23}$$

where n is the number of inclusions per unit volume and α_{mm} is the magnetic polarizability of the individual magnetic inclusion defined as [22]

$$\alpha_{mm} = -j\omega\mu_0 \frac{\ell^2}{Z_{\text{eff}}}. \tag{24}$$

The effective impedance associated to the individual magnetic inclusion Z_{eff} can be determined through the proposed circuits shown in Figs. 1(b), 3(b), and 5(b) for the multiple split-ring, spiral, and labyrinth resonator, respectively,

$$\begin{aligned} Z_{\text{eff}} = R_c^A + \frac{R_d^A}{1 + \omega^2 \left(C^A R_d^A \right)^2} \\ + j\omega \left[L^A - C^A \frac{\left(R_d^A \right)^2}{1 + \omega^2 \left(C^A R_d^A \right)^2} \right], \\ \text{with } A = \text{MSRR}, \text{SR}, \text{LR}. \end{aligned} \tag{25}$$

The analytical expression of the permeability derived through (23) is compared here with the permeability function derived through a direct numerical retrieval from the calculated scattering parameters [15], [16]. The corresponding results for the case of a multiple split-ring and a spiral resonator are reported in Figs. 8 and 9, respectively.

The results obtained through the employment of analytical formula (23), which is based on the models derived in Section II, are in a rather good agreement with the numerical data retrieved from the calculated scattering parameters.

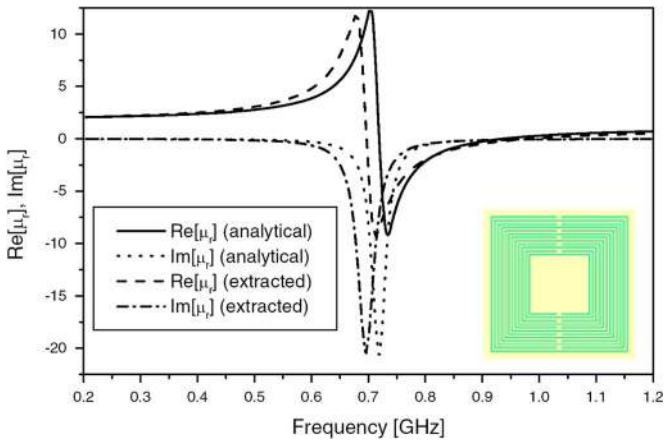

Fig. 8. Relative permeability of a multiple split-ring resonator medium as a function of frequency. Comparison between the analytical model proposed in this paper and the direct extraction from S-parameters. Data: $N = 12, \ell = 8$ mm, $w = 0.1$ mm, $s = 0.1$ mm, $t = 30\ \mu$m, $h = 0.2$ mm, $\varepsilon_r = 3.85, \tan\delta = 0.01, \rho_c = 0.017 \cdot 10^{-6}\ \Omega$m, $n = 1/8.8$ mm $\times$ 8.8 mm $\times$ 4.2 mm.

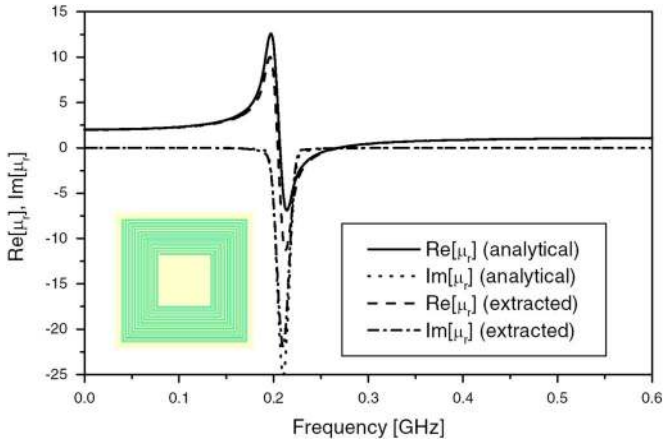

Fig. 9. Relative permeability of a spiral resonator medium as a function of frequency. Comparison between the analytical model proposed in this paper and the direct extraction from S-parameters. Data: $N = 12, \ell = 8$ mm, $w = 0.1$ mm, $s = 0.1$ mm, $t = 30\ \mu$m, $h = 0.2$ mm, $\varepsilon_r = 3.85, \tan\delta = 0.01, \rho_c = 0.017 \cdot 10^{-6}\ \Omega$m, $n = 1/8.8$ mm $\times$ 8.8 mm $\times$ 4.2 mm.

IV. Conclusion

In this paper, we have presented accurate analytical circuit models for the design of different magnetic inclusions, such as the multiple split-ring, spiral, and labyrinth resonators, to implement real-life metamaterials with anomalous values of the permeability. Starting from existing models considering only lossless metallic conductors and inclusions immersed in air, we have derived a complete formulation, which is able to take into account the presence of a dielectric substrate, where the inclusions are printed on and the presence of the losses in both the dielectric substrate and in the metallic conductor. The extended models presented here are able to predict with a very good accuracy the resonant frequency of individual multiple split-ring, spiral, and labyrinth resonators.

Moreover, the complete circuit model allows to derive an analytical expression of the quality factor of the individual inclusions, thus giving an estimation of the bandwidth of operation

of the corresponding metamaterial sample. The circuit models presented here also allow to analytically determine an expression of the permeability function, which has been shown to be in good agreement with the commonly used numerical retrieval techniques. The results obtained through the employment of the proposed models have been compared to both full-wave numerical results and to the measurements, showing good agreement.

REFERENCES

[1] H. Mosallaei and K. Sarabandi, "Magneto-dielectrics in electromagnetics: Concept and applications," *IEEE Trans. Antennas Propag.*, vol. 52, no. 6, pp. 1558–1567, Jun. 2004.

[2] A. Alù and N. Engheta, "Pairing an epsilon-negative slab with a mu-negative slab: Anomalous tunneling and transparency," *IEEE Trans. Antennas Propag.*, vol. 51, no. 10, pp. 2558–2570, Oct. 2003.

[3] A. Alù, F. Bilotti, N. Engheta, and L. Vegni, "Compact leaky-wave components using metamaterials," in *IEEE MTT-S Int. Microw. Symp. Dig.*, Long Beach, CA, Jun. 12–17, 2005, [CD ROM].

[4] A. Ishimaru, L. Seung-Woo, Y. Kuga, and V. Jandhyala, "Generalized constitutive relations for metamaterials based on the quasi-static Lorentz theory," *IEEE Trans. Antennas Propag. (Special Issue)*, vol. 51, no. 10, pp. 2550–2557, Oct. 2003.

[5] L. Landau and E. M. Lifschitz, *Electrodynamics of Continuous Media*. Oxford, U.K.: Pergamon, 1984.

[6] F. Bilotti, "Application of metamaterials for miniaturized components," presented at the Metamater. Ind., Jouy-en-Josas, France, Nov. 28–30, 2005, Short Course for Ind. and SMEs.

[7] A. Alù, F. Bilotti, N. Engheta, and L. Vegni, "Sub-wavelength, compact, resonant patch antennas loaded with metamaterials," *IEEE Trans. Antennas Propag.*, vol. 55, no. 1, pp. 13–25, Jan. 2007.

[8] R. W. Ziolkowski and A. D. Kipple, "Application of double negative materials to increase the power radiated by electrically small antennas," *IEEE Trans. Antennas Propag.*, vol. 51, no. 10, pp. 2626–2640, Oct. 2003.

[9] N. Engheta, "An idea for thin subwavelength cavity resonators using metamaterials with negative permittivity and permeability," *IEEE Antennas Wireless Propag. Lett.*, vol. 1, no. 1, pp. 10–13, 2002.

[10] F. Martín, F. Falcone, J. Bonache, T. Lopetegi, R. Marqués, and M. Sorolla, "Miniaturized coplanar waveguide stopband filters based on multiple tuned split ring resonators," *IEEE Microw. Wireless Compon. Lett.*, vol. 13, no. 12, pp. 511–513, Dec. 2003.

[11] J. B. Pendry, A. J. Holden, D. J. Robbins, and W. J. Stewart, "Magnetism from conductors and enhanced nonlinear phenomena," *IEEE Trans. Microw. Theory Tech.*, vol. 47, no. 11, pp. 2075–2081, Nov. 1999.

[12] F. Bilotti, A. Toscano, and L. Vegni, "Design of spiral and multiple split-ring resonators for the realization of miniaturized metamaterial samples," *IEEE Trans. Antennas Propag.*, to be published.

[13] K. Aydin, I. Bulu, K. Guven, M. Kafesaki, C. M. Soukoulis, and E. Ozbay, "Investigation of magnetic resonances for different split-ring resonator parameters and designs," *New J. Phys.*, vol. 7, no. 168, pp. 1–15, 2005.

[14] F. Bilotti, A. Toscano, L. Vegni, K. Aydin, K. M. Alici, and E. Ozbay, "Theoretical and experimental analysis of magnetic inclusions for the realization of metamaterials at different frequencies," in *IEEE MTT-S Int. Microw. Symp. Dig.*, Honolulu, HI, Jun. 3–8, 2007, pp. 1835–1838.

[15] D. R. Smith, D. C. Vier, T. Koschny, and C. M. Soukoulis, "Electromagnetic parameter retrieval from inhomogeneous metamaterials," *Phys. Rev. E, Stat. Phys. Plasmas Fluids Relat. Interdiscip. Top.*, vol. 71, pp. 1–11, 2005, 036617.

[16] X. Chen, T. Gregorczyk, B.-I. Wu, J. Pacheo, Jr., and J. A. Kong, "Robust method to retrieve the constitutive effective parameters of metamaterials," *Phys. Rev. E, Stat. Phys. Plasmas Fluids Relat. Interdiscip. Top.*, vol. 70, pp. 1–7, 2004, 016608.

[17] K. Buell, H. Mosallaei, and K. Sarabandi, "A substrate for small patch antennas providing tunable miniaturization factors," *IEEE Trans. Microw. Theory Tech.*, vol. 54, no. 1, pp. 135–146, Jan. 2006.

[18] J. D. Baena, R. Marques, F. Medina, and J. Martel, "Artificial magnetic metamaterial design by using spiral resonators," *Phys. Rev. B, Condens. Matter*, vol. 69, pp. 1–5, 2004, 014402.

[19] F. Bilotti, A. Alù, N. Engheta, and L. Vegni, "Miniaturized circular patch antenna with metamaterial loading," in *Proc. 1st Eur. Antennas Propag. Conf.*, Nice, France, Nov. 6–10, 2006, [CD ROM].

[20] F. Bilotti, A. Alù, N. Engheta, and L. Vegni, "Compact microwave absorbers utilizing single negative metamaterial layers," in *Proc. IEEE AP-S Int. Symp./USNC/URSI Nat. Radio Sci. Meeting*, Albuquerque, NM, 2006, [CD ROM].

[21] S. Ramo, J. R. Whinnery, and T. Van Duzer, *Fields and Waves in Communication Electronics*. New York: Wiley, 1994.

[22] P. Ikonen, "Artificial electromagnetic composite structures in selected microwave applications," Ph.D. dissertation, Radio Lab., Helsinki Univ., , Helsinki, Finland, 2007.

Filiberto Bilotti (S'97–M'03–SM'06) was born in Rome, Italy, on April 25, 1974. He received the Laurea (*summa cum laude*) and Ph.D. degrees in electronic engineering from the University of "Roma Tre," Rome, Italy, in 1998 and 2002, respectively.

Since 2002, he has been with the Department of Applied Electronics, University of "Roma Tre," where he is currently an Assistant Professor of electromagnetic field theory. He has authored or coauthored approximately 200 papers in international journals and conference proceedings. Since 2003, he has been a Technical Reviewer of the European Community for scientific projects in the fields of metamaterials and antennas. He is a member of the Editorial Board of *Metamaterials* and a Technical Reviewer for major international journals related to electromagnetic field theory. His main research interests are microwave applications of complex media, metamaterials and metasurfaces, analysis and synthesis of planar and conformal integrated components and phased antenna arrays, and development of improved numerical algorithms for an efficient analysis of printed antennas and circuits.

Dr. Bilotti has been a national expert of the European actions COST260 and COST284 on antenna technology and design (1999–2006). Since 2004, he has been a member of the governing bodies of METAMORPHOSE, the European Network of Excellence on Metamaterials, where he acts as the coordinator of spreading activities, with a particular emphasis on training events. He is also a member of the Steering Committee, European Doctoral School on Metamaterials. He served as a member of the Technical Program, Steering Committee, and Organizing Committee of several national and international conferences and training events related to metamaterials, and as organizer and chairman of special sessions focused on the applications of metamaterials at microwave frequencies. He was the recipient of the 2007 Raj Mittra Travel Grant Senior Researcher Award.

Alessandro Toscano (M'90) was born in Capua, Italy, on June 26, 1964. He received the Electronic Engineering degree and Ph.D. degree from the University of Rome "La Sapienza," Rome, Italy, in 1988 and 1993, respectively.

Since 1993, he has been with the Department of Applied Electronics, University "Roma Tre," Rome, Italy, where he is currently an Associate Professor. His research interests are microwave and millimeter-wave circuits and antennas, electromagnetic compatibility, and general techniques in electromagnetics of complex material media such as metamaterials.

Lucio Vegni (M'73) was born in Castiglion Fiorentino, Italy, on June 20, 1943. He received the Electronic Engineering degree from the University of Rome, Rome, Italy.

Following a period as an Antenna Designer with Standard Elektrik Lorenz, Stuttgart, Germany, he joined the Istituto di Elettronica, University of Rome, where he was a Researcher in applied electronics. From 1976 to 1980, he was Researcher Professor of applied electronics with the University of L'Aquila. From 1980 to 1985, he was a Researcher Professor of applied electronics, and from 1985 to 1992, he was an Associate Professor of electromagnetic compatibility with the University of Rome "La Sapienza." Since 1992, he has been with the University of "Roma Tre," Rome, Italy, where he is currently a Full Professor of electromagnetic field theory. He has authored or coauthored over 500 international papers appearing in journals,

transactions, and conferences. His research interests are in the areas of microwave and millimeter-wave circuits and antennas with a particular emphasis on electromagnetic compatibility problems. He was specifically active in studies on partial coherence radio links with particular attention on multipath electromagnetic propagation effects up until 1977. He then moved to the area of integrated microwave circuits, where he studied the electromagnetic modeling of microstrip planar circuits and antennas. In cooperation with industry, he was engaged in the development of integrated microstrip antennas for satellite applications and in study of radiating system electromagnetic compatibility problems from 1985 to 1990. Since 1990, he has been actively involved with theoretical and numerical aspects of new planar antennas modeling involving unconventional materials. In these recent studies, he has offered new contributions to equivalent-circuit representations of planar microwave components and new variational formulations for their numerical simulations. Finally, in the area of unconventional materials, he has given noteworthy contributions to the study of chiral and omega grounded dielectric slab antennas. His recent research activities are in the field of metamaterials.

Prof. Vegni has been the organizer and chairman of the second and third edition of the International Workshop on Metamaterials and Special Materials for Electromagnetic Applications and TLC, Rome, Italy (2004 and 2006). He is the local chairman of Metamaterials 2007—The First International Congress on Advanced Electromagnetic Materials in Microwaves and Optics, Rome, Italy (2007). He is a member of the European Chiral Group, the Network of Excellence METAMORPHOSE, and the Italian Electrical and Electronic Society (AEI).

Koray Aydin (S'03) was born in Ankara, Turkey, on April 10, 1980. He received the B.S. and M.S. degrees in physics from Bilkent University, Ankara, Turkey, in 2002 and 2004, respectively, and is currently working toward the Ph.D.. degree in physics at Bilkent University. His M.S. thesis focused on the characterization of left-handed metamaterials and negative refractive media.

He has authored or coauthored 28 refereed journal papers and 26 conference proceedings and abstracts. His research activities are conducted at the Nanotechnology Research Center, Bilkent University, Bilkent, Turkey. His research interests are left-handed metamaterials, sub-wavelength imaging and resolution, resonances in split-ring resonator structures, tunable metamaterials and negative refractive index in photonic crystals. He is listed in *Who's Who in Science and Engineering*.

Mr. Aydin is a member of the Optical Society of America (OSA), the IEEE Antennas and Propagation Society (IEEE AP-S), and The International Society for Optical Engineers (SPIE). He was the recipient of a 2007 SPIE Educational Scholarship.

Kamil Boratay Alici was born in Sivas, Turkey, on January 12, 1981. He received THE B.S. degree in physics from Bilkent University, Ankara, Turkey in 2004, and is currently working toward the Ph.D. degree at Bilkent University.

He has authored or coauthored eight papers in scientific journals. His scientific interests are electromagnetic metamaterials: antenna and superlens applications, acoustic metamaterials, and negative refraction in photonic crystals.

Mr. Alici was the recipient of the Undergraduate Scholarship (2001–2004), and Graduate Scholarship (2004–2009) of The Scientific and Technological Research Council of Turkey (TUBITAK).

Ekmel Ozbay was born in Ankara, Turkey, on March 25, 1966. He received the B.S. degree in electrical engineering from the Middle East Technical University, Ankara, Turkey, in 1983, and the M.S. and Ph.D. degrees in electrical engineering from Stanford University, Stanford, CA, in 1989 and 1992, respectively. His doctoral dissertation concerned high-speed resonant tunneling and opto-electronic devices.

From 1992 to 1994, he was a Scientist with the Department of the Environment (DOE), Ames National Laboratory, Iowa State University, where he was involved in the area of photonic-bandgap materials. In 1995, he joined Bilkent University, Ankara, Turkey, where he is currently a Full Professor with the Department of Electrical and Electronics Engineering and the Department of Physics. He is the Founding Director of the Nanotechnology Research Center, Bilkent University. He has authored or coauthored over 320 papers in scientific journals, conference proceedings, and books. His research involves nanophotonics, metamaterials, MOCVD growth and fabrication of GaN-based electronic and photonic devices, photonic crystals, and high-speed opto-electronics. He has been a Topical Editor of *Optics Letters* since 2002.

Dr. Ozbay was the recipient of the 1997 Adolph Lomb Medal of the Optical Society of America and the 2005 European Union Descartes Science Award.